

## How to erase surface plasmon fringes

Aurelien Drezet\* and Andrey L. Stepanov, Andreas Hohenau, Harald Ditlbacher, Bernhard Steinberger, Nicole Galler, Franz R. Aussenegg, Alfred Leitner, Joachim R. Krenn

*Institute of Physics and Erwin Schrödinger Institute for Nanoscale Research,  
Karl-Franzens-University Graz, Universitätsplatz 5, A-8010 Graz, Austria*

### Abstract

We report the realization of a dual surface plasmon polariton (SPP) microscope based on leakage radiation (LR) analysis. The microscope can either image SPP propagation in the direct space or in the Fourier space. This particularity allows in turn manipulation of the LR image for a clear separation of different interfering SPP contributions present close to optical nanoelements .

arXiv:1002.0791v1 [physics.optics] 3 Feb 2010

---

\*Electronic address: aurelien.drezet@uni-graz.at

The miniaturization of optical elements and devices into nanoscale dimensions is restricted by the diffraction limit to about half of the effective light wavelength. One promising way to avoid this restriction is the use of surface plasmon polaritons (SPPs) instead of light waves. SPPs are quasi-two-dimensional electromagnetic waves of electron excitations, propagating at a metal-dielectric interface and having field components decaying exponentially into both neighboring media [1]. As was recently demonstrated [2–4], to image the spatial SPP profile, besides near-field optical microscopy [5] or fluorescence mapping [6], leakage radiation (LR) imaging microscopy can be applied. It was shown that this new approach allows for quantitative measurements of the spatial SPP field profile by deducing SPP reflection, transmission, and scattering efficiencies for various surface nanostructures [4, 7]. In parallel to this LR microscopy in the direct space it has been recently experimentally demonstrated that LR imaging is equivalently possible in the Fourier space [8], e. g., imaging in the SPP wavevector space. Here, based on the use of a dual LR microscopy working in both the direct and Fourier space, we present the next development of LR imaging microscope and we discuss new possibilities for imaging and controlling of SPPs. In particular we show how by acting in the Fourier space this method can be applied to erase from the final image in the direct space SPP interferences fringes existing close to structure like Bragg mirror [6, 7]. This in turn allows quantitative analysis in a spatial region where near field optics can not resolve and distinguish the different SPP field components contributing to the SPP image.

The intensity decay length of a plane SPP wave in a perfectly planar metal film between two dielectric media defines its intrinsic decay length  $L_{\text{SPP}} = 1/2k''_{\text{SPP}}$ , which is a measure of the "ideality" of the electron gas.  $k''_{\text{SPP}}$  is defined as the imaginary part of the complex SPP wave vector  $k_{\text{SPP}} = k'_{\text{SPP}} + ik''_{\text{SPP}}$ . Intrinsic losses are caused by inelastic scattering of conduction electrons, scattering of electrons at interfaces and leakage radiation LR [1]. LR is emitted from the interface between a metal thin film and the higher refractive index medium (glass substrate) [4, 7]. When the electromagnetic SPPs field cross the metal film and reach the substrate, LR appears at a characteristic angle of inclination  $\theta_{LR}$  with respect to the interface normal. At this angle the LR wave satisfies  $k'_{\text{SPP}} = 2\pi/\lambda_{SPP} = nk_0 \sin\theta_{LR}$ , where  $nk_0$  is the wave vectors of LR,  $n$  being the refractive index of the glass substrate, and  $\lambda_{SPP}$  the SPP wavelength. Although LR contributes to SPP damping, it permits the direct mapping of the SPP propagation at the air/metal interface. Indeed, the intensity collected at any point  $P'$  of the image plane  $\Sigma'$  of the LR microscope with a charged-coupled-device

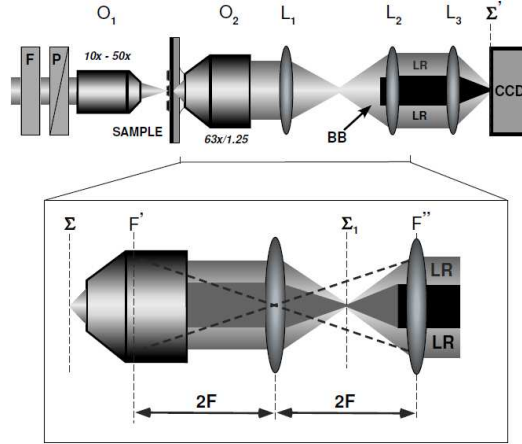


FIG. 1: Experimental scheme for Leakage Radiation (LR) imaging. SPPs are excited by laser light on a structured gold film on a glass substrate. LR is emitted into the glass substrate at an angle  $\theta_{LR}$ . F, gray filter; P, polarizer; BB, beam block.

(CCD) camera is directly proportional to the intensity of SPPs at the conjugate point  $P$  located on the air/metal boundary, i. e. , in the object plane  $\Sigma$  of the microscope. [4, 7]. The new LR microscope with the improvements discussed in the following is sketched on

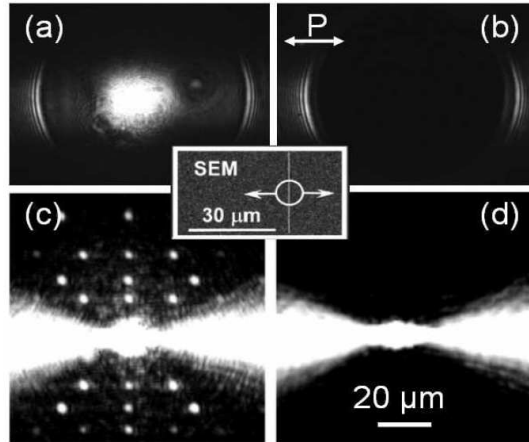


FIG. 2: LR Fourier plain images measured with blocked central beam (left) and without blocking (right). P shows the laser polarization direction.

Fig. 1. Like in the previous version of the LR microscope [4, 7] and in order to avoid total internal reflection inside the glass substrate, an oil immersion objective  $O_2$   $63\times$ , numerical aperture of 1.25) in contact with the bottom part of the sample is used to collect LR images.

It is important to remark that simultaneously to LR the incident exiting laser beam is going through the sample and the microscope contributing subsequently to the total signal in the  $\Sigma'$  plane. This direct laser light dominates the SPP signal in the region of excitation in  $\Sigma$ . This feature is conserved in  $\Sigma'$  where some distortions due to saturation of the camera are even added to the resulting image. It is consequently impossible to separate SPPs propagation from the incident beam in the vicinity of the excitation region. However, as well known from Fourier optics one can distinguish these two contributions by observing the intensity distribution in the back focal plane  $F'$  of the immersion objective. Indeed since the signal collected in  $F'$  is a cartography of the 2D momentum distribution of photons emitted in  $\Sigma$  the SPP distribution is thus confined on a circle corresponding to  $k'_{SPP}$ . Additionally, the central beam (with an angular divergence much smaller than  $\theta_{LR}$ ) is located at the center of this circle. By introducing a central beam-block in  $F'$  it is then possible to eliminate the direct contribution of the laser beam. By contrast with the previous version of LR microscope [4] we included this beam block in the optical setup. Since however  $F'$  is contained in the immersion objective we must first image  $F'$ , in a plane  $F''$ , by using a lens  $L_1$  in a 2f-2f configuration. In  $F''$  we can introduce the central beam-block (see Fig. 1). In order to image the SPP propagation in the direct space we introduce two auxiliary lenses  $L_2$  and  $L_3$  focusing light on the CCD ( $L_2$  is located in  $F''$ ). By changing the focal length of  $L_3$  one can either image the Fourier plane  $F''$  or the object plane  $\Sigma_1$  (image of  $\Sigma$  through  $O_2$  and  $L_1$ ). This dual microscope is consequently able of recording SPPs propagation either in the direct or in the Fourier space.

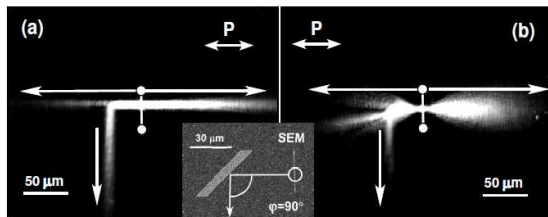


FIG. 3: LR images of SPPs launched from a ridge and interacting with a Bragg mirror (SEM structure in the inset). SPPs impinge at  $45^\circ$  incidence on the Bragg mirror (optimized for this angle at  $\lambda = 800$  nm). (a) Image with  $O_1 = (10\times, \text{numerical aperture } 0.25)$ . (b) Image with  $O_1 = (50\times, \text{numerical aperture } 0.7)$ . P shows the laser polarization direction.

In order to illustrate the potentiality of this optical setup we consider different nanos-

structures obtained by usual electron beam lithography (EBL) [9] on a 60 nm thick gold film. For the local excitation of SPPs we focus a linearly polarized light from a Ti:sapphire laser (wavelength:  $\lambda = 800 \simeq \lambda_{SPP}$  nm) through a microscope objective  $O_1$  onto a gold ridge (200 nm wide, 60 nm high). Launched SPPs propagate to the left and to right of the ridge in the direction perpendicular to the ridge axis. Figs. 2a, b, c, d show LR images of SPPs corresponding to this configuration ( $O_1:50\times$ , numerical aperture 0.7). Figs. 2a and c correspond to imaging in the Fourier and direct space respectively. The central spot associated with the laser beam and the partial ring associated with the SPPs cone are clearly visible on Fig. 2a. This laser beam saturates the image in the direct space and creates some artefact in the launching region as visible on Fig. 2c. Figs. 2b,d show the same images with the central beam block introduced in the plane  $F'$ . As a consequence of this introduction the multiple artefact disappear from the image in the direct space resulting in improvements of image quality and eliminating the spurious effect of the incident laser light (see Fig. 2d).

As a further modification, we introduced the use of different objectives for focusing of the laser beam. The different focus diameters achievable with the various objectives of focal length  $f_1$  allow in turn the generation of SPP waves of different divergence angles. Indeed the convergence angle  $\alpha$  of the laser beam on the sample is connected to the laser beam diameter  $W \simeq 2$  mm just before the lens by the relation  $\tan(\alpha) = W/(2f_1)$ . Due to Heisenberg's relation we have in the sample plane  $\tan(\alpha) = 2\lambda/(\pi W_0)$  where  $W_0$  is the focus beam diameter in the sample plane. Since SPPs launched from the ridge obey to the same Heisenberg relation we conclude that the divergence angle of the SPP beam equals  $\arctan[(\lambda/\lambda_{SPP}) \cdot \tan(\alpha)] \simeq \alpha$ , i. e. the convergence angle of the laser beam. This principle is illustrated in Fig. 3 which shows LR images of SPPs launched by a ridge and reflected by a Bragg mirror [5–7]. The Bragg mirror considered here has been optimized for  $45^\circ$  incidence angle with respect to the direction normal to Bragg's mirror in the sample plane. The mirror is made of gold ridges (60 nm height, 140 nm wide) separated by a distance  $\lambda_{SPP}/\sqrt{2} \simeq 556nm$  as described in [5]. Comparison of Fig. 3a ( $O_1: 10\times$ , NA=0.25) with Fig. 3b ( $O_1: 50\times$ , NA=0.7) show clearly that the Bragg mirror is much more efficient with a parallel beam ( $\alpha = 2^\circ$ , see Fig. 3a) that with a divergent beam ( $\alpha = 18^\circ$ , see Fig. 3b). This method of generating a parallel SPPs beam can be considered as an alternative to prism technics used in PSTM imaging [5]. The black shadow in the transmitted beam of Fig. 3b shows directly in counterpart the reflectivity acceptance angle of the Bragg mirror. Both

approach can be thus useful for understanding SPPs reflectivity of such system. Additionally it must be added that in order to observe SPPs reflectivity with a narrow beam like in Fig. 3a the use of the central beam block is necessary. Indeed without this beam block the laser beam of diameter  $W_0 \simeq 15 \mu\text{m}$  would saturate the recorded signal in the region of interest between the ridge and the Bragg mirror. The effect is less pronounced for divergent beam  $\alpha = 18^\circ$  where  $W_0 \simeq 2 \mu\text{m}$ .

It should be however remarked that the potentiality of such a dual LR microscope are not

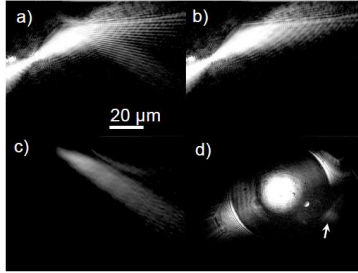


FIG. 4: LR images of SPPs launched from a ridge and interacting with a Bragg mirror like the one in Fig. 3. SPPs impinge at  $60^\circ$  incidence on the Bragg mirror ( $\lambda = 800 \text{ nm}$ ). SPP interference fringes are visible close to the Bragg mirror. (b) LR image of SPPs propagation in the direct space ( $O_1$ :  $10\times$ ,  $\text{NA}=0.25$ ). (b) LR image of the incident SPP wave launched from the ridge region. (c) LR image of the reflected SPP beam. Fringes are removed from (b) and (c). LR image of SPPs in the Fourier plane  $F''$  without beam block. The introduction of beam blocks in  $F''$  (not shown) give rises to figures (b) and (c). The arrow shows the reflected beam in  $F''$ .

limited to correction of artefact or improvement in LR images quality. Indeed the definition of Fourier optics itself allow us to manipulate the images in order to extract some relevant physical information hidden in the pictures. This is illustrated in Fig. 4 which shows LR images of SPP reflected at large incidence angle (e. g. ,  $\theta_{\text{inc}} = 66^\circ$ ) on a Bragg mirror like the one shown in Fig. 3. Interference between the incident and reflected SPP field give rises to fringes in the region close to the mirror (see Fig. 4a). The presence of interference prohibit a simple and direct analysis of SPP reflection. However as shown in Fig. 4d the LR image in the Fourier space separates clearly the respective contributions of the incoming laser beam (the central spot), of the incident SPP launched from the ridge (the two arcs of circle), and of the reflected SPP beam (indicated by an arrow). By positioning adequately a beam block in this Fourier plane one can remove not only the incoming laser beam but selectively image

either the incident and transmitted beams (see Fig. 4b) or the reflected beam (see Fig. 4c) alone. The interference fringes are clearly erased from the LR pictures. This method in turn allow direct quantitative analysis not directly possible with the previous existing methods [4–6].

In summary, Thus, based on conventional microscopy dual LR imaging proves to be a quick and reliable technique for probing SPP fields with the advantage of providing possible quantitative analysis in both Fourier and direct space. This dual method is particularly adapted to analysis of SPP propagation in region where different beams interfere and where different contributions can thus be selectively erased for subsequent analysis.

The authors thank M.U. González for test-sample preparation. For financial support, the European Union under projects FP6 NMP4-CT-2003-505699, FP6 2002-IST-1-507879 and the Lisa Meitner programm of the Austrian Scientific Foundation (M868-N08) are acknowledged.

- 
- [1] H. Raether, *Surface Plasmons*(Springer, Berlin, 1988).
  - [2] B. Hecht, H. Bielefeldt, L. Novotny, Y. Inouye, and D. W. Pohl, *Phys. Rev. Lett.* **77**, 1889 (1996).
  - [3] A. Bouhelier, Th. Huser, H. Tamaru, H.-J. Güntherodt, D. W. Pohl, F.I. Baida, D. Van Labeke *Phys. Rev. B* **63**, 155404 (2001).
  - [4] A. Stepanov, J. R. Krenn, H. Ditlbacher, A. Hohenau, A. Drezet, B. Steinberger, A. Leitner, and F. Aussenegg, *Opt. Lett.* **30**,1524 (2005).
  - [5] J.-C. Weeber, M. U. González, A.-L. Baudrion, and A. Dereux, *Appl. Phys. Lett.* **87**, *Appl. Phys. Lett.* **87**, 1 (2005).
  - [6] H. Ditlbacher, J. R. Krenn, G. Schider, A. Leitner, and F. R. Aussenegg, *Appl. Phys. Lett.* **81**, 1762 (2002).
  - [7] A. Drezet, A. L. Stepanov, H. Ditlbacher, A. Hohenau, B. Steinberger, F. R. Aussenegg, A. Leitner, and J. R. Krenn, *Appl. Phys. Lett.* **86**, 074104 (2005).
  - [8] W. L. Barnes, *Opt. Express* **13**, 428 (2005).
  - [9] A. Hohenau, H. Ditlbacher, B. Lamprecht, J. R. Krenn, A. Leitner, F. R. Aussenegg, to appear in *Microelec. Engin.* (2006).